HHS Public Access

Author manuscript

Stem Cells. Author manuscript; available in PMC 2018 April 05.

Published in final edited form as:

Stem Cells. 2016 April ; 34(4): 1097–1111. doi:10.1002/stem.2325.

Serially transplanted non-pericytic CD146⁻ Adipose Stromal/ Stem Cells in silk bioscaffolds regenerate adipose tissue *in vivo*

Trivia P. Frazier, Ph.D.[a], **Annie Bowles**[a], **Stephen Lee**[b], **Rosalyn Abbott**[f], **Hugh A. Tucker**[a], **David Kaplan, Ph.D.**[f], **Mei Wang**[b], **Amy Strong, Ph.D.**[a], **Quincy Brown**[b], **Jibao He**[b], **Bruce A. Bunnell, Ph.D.**[a,c], and **Jeffrey M. Gimble, M.D., Ph.D.**[b,d,e]

[a]Center for Stem Cell Research and Regenerative Medicine, Tulane University School of Medicine, New Orleans, LA, USA

[b]Department of Biomedical Engineering, Tulane University, New Orleans, LA, USA

[c]Department of Pharmacology, Tulane University School of Medicine, New Orleans, LA, USA

[d]Departments of Medicine, Structural and Cellular Biology, and Surgery, Tulane University School of Medicine, New Orleans, LA, USA

[e]LaCell, LLC., New Orleans Bio-innovation Center, New Orleans, LA, USA

[f]Departments of Biomedical Engineering and Chemical Engineering, Tufts University, New Orleans, LA, USA

Abstract

Progenitors derived from the stromal vascular fraction (SVF) of white adipose tissue (WAT) possess the ability to form clonal populations and differentiate along multiple lineage pathways. However, the literature continues to vacillate between defining adipocyte progenitors as “stromal” or “stem” cells. Recent studies have demonstrated that a non-pericytic subpopulation of adipose stromal cells, which possess the phenotype, $CD45^{-}/CD31^{-}/CD146^{-}/CD34^{+}$, are mesenchymal, and suggest this may be an endogenous progenitor subpopulation within adipose tissue. We hypothesized that an adipose progenitor could be sorted based on the expression of CD146, CD34, and/or CD29 and when implanted *in vivo* these cells can persist, proliferate, and re-generate a functional fat pad over serial transplants. Stromal vascular fraction (SVF) cells and culture expanded adipose stromal/stem cells (ASC) ubiquitously expressing the GFP transgene (GFP-Tg) were fractionated by flow cytometry. Both freshly isolated SVF and culture expanded ASC were seeded in 3-dimensional silk scaffolds, implanted subcutaneously in wild type hosts, and serially transplanted. Six week WAT constructs were removed and evaluated for the presence of GFP-Tg adipocytes and stem cells. Flow cytometry, quantitative polymerase chain reaction, and confocal microscopy demonstrated GFP-Tg cell persistence, proliferation, and expansion, respectively.

Authors’ Contributions

All co-authors have contributed significantly to the production of this manuscript. AB, AS, and SL were instrumental in executing planned experiments. RA and DK graciously provided synthesized HFIP-based silk scaffolds for cell seeding and serial transplantation studies. HT performed flow cytometry and fluorescence-activated cell sorting experiments within the flow cytometry core facility. MW and QB provided access to Zenalux Zenascope instrumentation, training, and access to raw data for hemoglobin comparison analyses within cohorts. JH performed cryo-SEM studies. TF performed all other experiments within the study and drafted the manuscript. BAB and JG both developed the aims of the studies and were instrumental in finalization of the manuscript. All co-authors read and approved the final manuscript.

Glycerol secretion and glucose uptake assays revealed GFP-Tg adipose was metabolically functional. Constructs seeded with GFP-Tg SVF cells or GFP-Tg ASC exhibited higher SVF yields from digested tissue, and higher construct weights, compared to non-seeded controls. Constructs derived from $CD146^{-}$ $CD34^{+}$ -enriched GFP-Tg ASC populations exhibited higher hemoglobin saturation, and higher frequency of GFP-Tg cells than unsorted or $CD29^{+}$ GFP-Tg ASC counterparts. These data demonstrated successful serial transplantation of non-pericytic adipose derived progenitors that can reconstitute adipose tissue as a solid organ. These findings have the potential to provide new insights regarding the stem cell identity of adipose progenitor cells.

Introduction

The term “stem cell” was first introduced by nineteenth century embryologists to describe the germline lineages and, shortly thereafter, was associated with the development of the hematopoietic system[1]. A true “stem” cell, as demonstrated by the classical adult hematopoietic stem cell (HSC) model, is defined as possessing the ability to differentiate along lineage specific pathways and to self-renew *in vivo*[1,2]. Only a decade ago, investigators believed that bone marrow was the only adult tissue site that contained stem cells; however, multiple studies of adipose tissue have challenged this paradigm. In 2006, the International Society for Cellular Therapy (ISCT)[3] issued a statement regarding the definition of MSC, where the acronym is specifically defined as “multipotent stromal cells” rather than “mesenchymal stem cells” to avoid the use of “stem” as a terminology. Specifically within adipose, in vitro studies have documented the ability to isolate progenitor cells from the stromal vascular fraction (SVF) of human subcutaneous white adipose tissue (WAT). These cells can form clonal populations and differentiate along multiple lineage pathways[3–6]. Adipose-derived progenitors expressed “stem” cell associated surface antigens (CD34) and transcription factors (Oct4, Sox2)[5–7]. While some argue that the progenitors in adipose tissue derive from bone marrow depots as a circulating population[8–10], there is ample data supporting the presence of an endogenous progenitor subpopulation within the adipose tissue itself[11–13]. Multiple studies have attempted to isolate and characterize this progenitor population, and a subset have reported data suggesting that these cells are a non-pericytic subpopulation within the SVF and are associated with a $CD34^{+}/CD29^{+}$ $CD146^{-}$ phenotype. Nevertheless, the literature continues to waver between defining adipocyte progenitors as “stromal” vs. “stem” cells[3, 4,14]. Over the past decade, there has been a good deal of controversy at the scientific and public level associating the term “stem” exclusively with pluripotent cells derived from embryos, rather than with cells from adult tissues. Thus, the question remains whether the adipose-derived progenitor cell is a “stromal” or “stem” cell.

The distinction between adipose progenitor cells as a “stromal” cell vs. a “stem” cell is multi-faceted and has considerable implications at the basic science, clinical, and translational levels. For example, a growing number of reconstructive surgeons are using autologous stromal vascular fraction (SVF) cells isolated from adipose tissue as an “off label” product for various purposes in the operating room[15–17]. Data from multiple studies supports the premise that multipotent stromal cells contained within the SVF accelerate

regeneration of injured tissue through their regulation and release of cytokine/chemokine growth factors post implantation[18–20]. Based on this evidence, cardiologists, neurologists and vascular surgeons are seeking to exploit the angiogenic cytokine secretory capacity of adipose-derived cells to treat myocardial infarction[21–23], stroke[24–26], and peripheral limb ischemia[27–31].

Furthermore, recent studies have demonstrated that a specific, non-pericytic subpopulation of adipose stromal cells within the SVF, which possess the phenotype, $CD45^{-}/CD31^{-}/CD146^{-}/CD34^{+}$, are highly mesenchymal in phenotype [(94.4 ± 3.2)% CD73+/CD105+, (95.5 ± 1.2)% CD90+][32]. These studies also suggest that a relationship exists between pericytes and this non-pericytic SVF subpopulation, with the $CD45^{-}/CD31^{-}/CD146^{-}/CD34^{+}$ GFP-Tg ASC being the most mesenchymal of SVF cells[32, 33]. To our knowledge, no studies have reported on the regenerative capacity of a flow sorted, non-pericytic ($CD146^{-}/CD34^{+}$) SVF subpopulation in a serial transplantation model that is similar to the original HSC model.

The aim of the current study was to investigate the self-renewal properties of a non-pericytic SVF subpopulation, and thereby determine the importance of stem cell self-renewal as a contributory mechanism for SVF cell and ASC function *in vivo*. Due to the unique association of CD146 with pericytes, and CD34 with ASC (as opposed to bone marrow derived mesenchymal stromal cells, BMSC) as well as with hematopoietic stem and progenitor cells, $CD146^{-}$, $CD34^{+}$ phenotypic expression was chosen for analysis of “stem-ness” within the study. In comparison, CD29, or beta 1 integrin, is an abundant surface antigen that has been associated with both ASC and BMSC functionality. Thus, we hypothesized that a labeled non-pericytic adipose progenitor could be sorted based on the expression of CD146, CD34, and/or CD29 and, when placed *in vivo*, could persist, proliferate, and generate a functional fat pad over serial transplants. The novelty of this study lies in the combination of transgenic labeled cell populations with 3-dimensional tissue engineered constructs for serial transplantation of adipose depots. Since “serial transplantation” has been a critical “gold standard” for the definition of hematopoietic stem cells and bone marrow transplantation for nearly 5 decades, the concept of serial transplantation of stem cells reconstituting adipose tissue as a solid organ has the potential to provide new insights regarding the stem cell identity of adipose progenitor cells.

Materials and Methods

Materials

Unless otherwise specified, all antibodies were purchased from eBioscience or Biolegend (San Diego, CA) and all chemicals were purchased from Sigma-Aldrich (St. Louis, MO) or Fisher Scientific (Norcross, GA).

Mice

Animal studies were performed under the veterinary supervision of the Department of Comparative Medicine of the Tulane University School of Medicine under a protocol reviewed and approved by the Institutional Animal Care and Use Committee in accordance

with federal, state, and National Institute of Health policies and regulations. SVF cells and ASC were isolated from 8–12 week male C57BL/6-Tg (UBC-GFP) 30cha/J mice (human ubiquitin C promoter driven GFP transgene, Jackson Laboratory, Bar Harbor ME) according to published methods[32]. GFP-Tg ASC retain expression of the GFP transgene upon isolation and *in vitro* expansion out to at least 10 passages, and display a cell doubling time of between 2 to 2.5 days. For initial characterization, cells were examined for expression of markers CD11b (Mac-1α; Integrin alpha M), CD29 (β1 integrin), CD34 (mucosialin), CD45 (leukocyte common antigen; Ly5), CD90 (Thy-1), and Sca-1 (stem cell antigen 1; Ly6A/E).

Adipose Tissue Harvest and SVF Cell Preparation

Subcutaneous inguinal white adipose tissue (iWAT) from 8–12 week male C57BL/6-Tg (UBC-GFP) 30cha/J mice was isolated, minced, and digested with collagenase for 60 minutes according to a published protocol from our laboratory[31]. Briefly, the iWAT SVF pellets were collected by centrifugation, washed in PBS, filtered through a 70 μm mesh (Millipore), and the SVF cell concentrations determined by automated Cell Countess (Invitrogen) count. The 1° SVF cells were suspended in Stromal Medium (DMEM/F-12 Ham's, 10% FBS [Hyclone, Logan, UT, http://www.hyclone.com], 100 U penicillin/ 100 g streptomycin/0.25 g fungizone) at a density of 0.156 ml of tissue digest/cm^2 of surface area for expansion and culture to get GFP-Tg ASC, or resuspended at a final concentration of 1×10^6 nucleated cells per mL in phosphate buffered saline (PBS), in preparation for staining.

SVF Cell Initial Immunophenotype and Subfractionation

Cell suspensions were incubated with antibodies against the cell surface antigens listed in the Supplementary Table at room temperature (RT) for 30 minutes, protected from light. After two washes with PBS, flow cytometric analysis was performed using a Beckman-Coulter Galios flow cytometer (BD Biosciences, San Jose, CA). The immunophenotype and relative subpopulations within the GFP-Tg SVF cells were determined out to passage 2 of plastic adherent culture using fluorochrome conjugated monoclonal antibodies detecting the following panel of endothelial, hematopoietic, mesenchymal, and stem cell associated antigens using the scheme provided in the Supplementary Table.

SVF Cell Selection

Two studies were performed that utilized GFP-Tg cells from GFP-Tg C57BL/6 mice (see Methods Figure). These include serial transplantation of GFP-Tg unfractionated SVF cells, and serial transplantation of live-cell sorted, culture expanded GFP-Tg ASC subpopulations. For the first study, GFP-Tg SVF cells were selected by flow sorting for the GFP-Tg population, and unfractionated GFP-Tg SVF cells were immediately loaded onto silk scaffolds for GFP-Tg SVF serial transplantation in non-GFP-Tg mice. For the second study, the GFP-Tg $CD146^-$ SVF subpopulation was selected and either plated as: a) unfractionated controls, or sorted based on b) CD29 positivity, and c) CD34 positivity. The culture-expanded populations (a–c) were immunophenotyped, and loaded onto silk scaffolds for GFP-Tg ASC serial transplantation (ASC serial transplantation studies; see *HFIP Silk Scaffold Loading, Culture, and Implantation* below).

ASC Culture Expansion

Live cell sorting of GFP-Tg 1° SVF cells was performed using a BD Biosciences fluorescence-activated cell sorter (FACS) Beckman-Coulter Galios flow cytometer with 2 lasers and 8 detectors running Galios acquisition software (BD Biosciences, San Jose, CA). All selected fluorochromes remained compatible with the continued use of the transgenic GFP for cell sorting purposes. Lineage depletion was performed using a cocktail of eFluor-conjugated antibodies detecting murine (mu) CD3, CD45R, CD116, LyG6, Ter-119 (eBioscience; 88–7772). Live SVF cell selection was performed with APC conjugated anti-muCD29 (17–0291) and PE conjugated anti-muCD34 (56–0341). ASC were isolated following plastic adherent culture expansion and using phenotypic and functional criterion established by International Federation of Adipose Therapeutics (IFATS) and the ISCT[3]. Briefly, passage 0 (P0) ASCs were subjected to trypsinization with 5 mL 0.25% trypsin (Life Technologies, Grand Isle, NY) for 5 minutes. Trypsin digestion was stopped by the addition of an equal amount of ASC culture medium. P0 ASCs were counted using trypan blue dye exclusion, and passaged in new T175 flasks at a density of 0.4×10^3 cells/cm^2. Cells were cultures until they reached 70% confluency. Populations were culture expanded to P2 as (a) unfractionated as controls or subfractionated into (b) a $CD29^+$ enriched population (Lin^- $CD29^+$ $CD146^-$) or (c) a $CD34^+$ enriched population (Lin^- $CD34^+$ $CD146^-$). The (a) unfractionated controls, (b) $CD29^+$ enriched ASC populations and (c) $CD34^+$ enriched ASC populations were individually seeded in flasks and culture expanded according to our published and validated methods[37]. After sorting for CD29, 95.05 ± 2% of the cells expressed CD29 and GFP. These SVF sub-populations were immediately plated, expanded, and passaged in order to get a sizeable population for seeding. Please note that the cells ($CD29^+$ and $CD34^+$ subpopulations) were selected separately, and were not sorted based on co-expression of both CD29 and CD34. In addition, the initial CD34 sorted subpopulation (*99.85 ± 4% positive for both GFP and CD34*) included other SVF precursor populations that may co- express CD34, and would be eliminated during plastic adherent expansion and selection of the adherent ASC populations; therefore, the initial sorted CD34 expression in SVF cells would be higher than that of culture-expanded CD34 selected ASCs, which may lose the expression of the surface marker as a function of the adherence and proliferative processes. At passage 2 (P2), an aliquot of the ASC (1×10^5 ASC) from each SVF fraction was characterized by analytical flow cytometry for GFP positivity and the antigens CD29, CD31, CD34, CD45, CD73, CD90, CD105, CD146, and Sca-1 to monitor changes in profile due to expansion[33]. In parallel, the live P2 GFP-Tg ASC were evaluated for proliferation, colony formation, and adipogenic differentiation *in vitro* or for implantation studies (see below).

HFIP Silk Scaffold Loading, Culture, and Implantation

The HexaFluoroIsoPropanol (HFIP) silk scaffolds obtained from the Tissue Engineering Resource Center, Tufts University were pre-wet overnight at 4° C in Stromal Medium (Dulbecco's modified Eagle's-Ham's F-12 medium supplemented with 10% fetal bovine serum, and 1% penicillin/streptomycin). The scaffolds were used in studies with unfractionated SVF cells, and with studies using fractionated passage 2 (P2) ASC. For the SVF study, the freshly isolated GFP-Tg iWAT 1° SVF cells were loaded by pipet in two aliquots of 50 μL each containing a total of 2.5×10^5 cells to opposite faces of a cylindrical

HFIP silk scaffold as per our published methods[33]. For the ASC study, a sample of freshly isolated GFP-Tg iWAT 1° SVF cells was directly plated (unfractionated), or sorted based on $CD146^{-}$ $CD29^{+}$ or $CD146^{-}/CD34^{+}$ expression. The subfractions were plated and cultured until P2. The P2 ASC derived from unfractionated SVF controls, $CD146^{-}$ $CD29^{+}$ enriched populations, and $CD146^{-}$ $CD34^{+}$ enriched populations were loaded by pipet in two aliquots of 50 μL each containing a total of 2.5×10^5 cells to opposite faces of a cylindrical HFIP silk scaffold.

For both studies, the scaffolds were transferred to a humidified 37° C, 5% CO_2 incubator and rotated every 15 min over a 2 hr. period. Following the addition of 5 ml of Stromal Medium, each scaffold was immediately implanted into 8-week male non-transgenic C57Bl/6 mice. A set of representative scaffolds (1° SVF cell or cultured ASC population) were retained, fresh frozen in OCT, and stored for use as positive controls. The remaining individual scaffolds loaded with SVF cells or ASC (n = 20 for each subpopulation) were implanted bilaterally into a dorsal subcutaneous pouch created in C57Bl/6 mice according to standard veterinary practices under an approved IACUC protocol (Protocol #4302). Each transplanted mouse was implanted with a randomized combination of empty scaffolds (control), those seeded with SVF cells, or P2 ASC that were unfractionated controls, $CD29^{+}$ enriched population ($CD29^{+}$ $CD146^{-}$), or $CD34^{+}$ enriched population ($CD34^{+}$ $CD146^{-}$).

Proliferation Assay

Immediately after cell seeding, the relative number of metabolically active stem cells within each seeded scaffold was determined by the AlamarBlue™ assay according to the manufacturer's instructions[34]. Seeded scaffolds were incubated in Stromal Medium supplemented with 10% Alamar Blue reagent for 2 hrs at 37°C with 5% CO_2. Aliquots (100 μl) of the culture medium were transferred to 96 well plates and quantified for fluorescence intensity with a microtiter plate reader (Fluostar Optima) using an excitation wavelength of 560 nm and an emission wavelength of 590 nm. Non-seeded scaffolds and tissue culture wells were also maintained in culture medium as above and were analyzed similarly as blank controls to adjust for background fluorescence. Scaffolds were then weighed and the relative cell numbers were calculated as the degree of their relative fluorescence intensity (RFU) per mg of scaffold wet weight as previously described[34].

Adipogenic Differentiation

Adipogenic differentiation of culture-expanded, and scaffold-seeded non-GFP-Tg ASC or GFP-Tg ASC was performed over a 15 day period as previously described[4]. Briefly, cultured ASC were grown in Stromal Medium (Dulbecco's modified Eagle's-Ham's F-12 medium supplemented with 10% fetal bovine serum, and 1% penicillin/streptomycin). ASC were then trypsinized and plated in 24-well plates in ASC culture media at 3×10^4 cells/cm^2 for 24 hrs to allow attachment. On day 1 (24 hours after plating), the medium was removed and cells were incubated for three days in adipogenic differentiation medium (Dulbecco's modified Eagle's-Ham's F-12 medium supplemented with 10% fetal bovine serum, 15 mM HEPES (pH 7.4), biotin (33 μM), pantothenate (17 μM, Sigma), human recombinant insulin (100 nM, Boehringer Mannheim), dexamethasone (1 μM), 1-methyl-3-isobutylxanthine (IBMX; 0.25 mM), and rosiglitazone (1 μM). For the remaining 9 days of the adipocyte

differentiation maintenance period, the medium was removed every 3 days and replaced with the same medium that did not contain IBMX and rosiglitazone (maintenance medium).

Adipogenesis of scaffold-seeded cells

For scaffold seeded GFP-Tg SVF cells and GFP-Tg ASC, one day prior to seeding, scaffolds were autoclaved and pre-soaked in adipogenic medium in 37°C, 5% CO_2, 95% relative humidity. GFP-Tg ASC were then trypsinized and plated loaded onto pre-soaked scaffolds in ASC adipogenic differentiation media by pipet in two aliquots of 50 μL each containing a total of 2.5×10^5 cells to opposite faces of a cylindrical HFIP silk scaffold as per published methods[33]. The cells were incubated for three days in adipogenic differentiation medium (Dulbecco's modified Eagle's-Ham's F-12 medium supplemented with 10% fetal bovine serum, 15 mM HEPES (pH 7.4), biotin (33 μM), pantothenate (17 μM, Sigma), human recombinant insulin (100 nM, Boehringer Mannheim), dexamethasone (1 μM), 1-methyl-3-isobutylxanthine (IBMX; 0.25 mM), and rosiglitazone (1 μM). For the remaining 9 days of the adipocyte differentiation maintenance period, the medium was removed every 3 days and replaced with the same medium that did not contain IBMX and rosiglitazone (maintenance medium). Similarly, control cultures were maintained in parallel in the absence of adipogenic stimulants. All seeded and nonseeded (control) scaffolds were cultivated in a humidified incubator at 37°C with 5% CO_2. Following the *in vitro* cultivation period, seeded scaffolds were evaluated for their extent of adipogenesis.

Intracytoplasmic Lipid Quantification

For plastic adherent cultured ASC, lipid formation was assessed by incorporation of Oil-Red-O (ORO) (Sigma-Aldrich) into monolayers of GFP-Tg ASC cultured in adipocyte differentiation medium for 12 days. Quantitation of ORO incorporation was performed as previously described[4]. Briefly, 0.5% (w/v) ORO was prepared in ethanol. 3 parts ORO and 2 parts PBS were then mixed to make a working solution. Monolayers of GFP-Tg ASC cultured in 12-well plates were rinsed 3 times with PBS and subsequently fixed in 10% (v/v) formalin (Sigma-Aldrich) for 15 minutes. The monolayers were then rinsed 3 times with PBS and then incubated in ORO working solution for 45 minutes at room temperature. Following aspiration of unincorporated ORO, monolayers were rinsed 4 times with PBS. Stained monolayers were visualized with phase contrast microscopy (Eclipse 800, Nikon; Tokyo, Japan). Incorporated ORO was extracted by incubating stained monolayers in 100% isopropanol for 10 minutes. The absorbance at 510 nm of each aliquot was then measured using a 96 well plate reader (Fluostar Optima, BMG Labtech).

For scaffold-loaded ASC, accumulated lipid was also visualized using ORO staining. Scaffolds were fixed in 2 M sucrose overnight for histology. The scaffolds were embedded in OCT medium, frozen over dry ice, and stored at −80°C. Frozen scaffolds were then sectioned (7-μm sections) using a cryostat and stained. For ORO staining, frozen sections were fixed in 10% buffered neutral formalin for 15 min, and rinsed with distilled water. ORO working solution was placed onto frozen sections and incubated for 20 min. Slides were rinsed with distilled water, and counterstained with DAPI according to manufacturer's protocol. Stained sections were covered using glass cover slips. Images were taken using phase contrast microscopy.

Serial Transplantation

The transplanted animals were maintained for 6–8 weeks, euthanized, and the scaffolds were removed using aseptic dissection techniques. Prior *in vivo* studies have demonstrated that 4–6 weeks is a sufficient period to allow for human ASC adipogenesis in transplanted silk scaffolds[33]. We observed a surge in GFP-Tg cell expansion and differentiation by confocal microscopy following 6 weeks. Therefore our studies were carried out to week 6. Sets of n = 2 scaffolds were fresh frozen in OCT for microscopic analyses. The remaining n =18 scaffolds were subjected to collagenase digestion for one hour in PBS supplemented with 0.1% collagenase type I (Worthington Biochemicals, Brunswich NJ), 1% bovine serum albumin, and 2 mM $CaCl_2$ for 60 min at 37°C with intermittent shaking. The 2° (secondary implanted) SVF cells were isolated as described above, under *HFIP Silk Scaffold*

Loading, Culture, and Implantation

The frequency of GFP-Tg cells in the 2° SVF as well as their expression of associated antigens (panel of mAbs above) were determined by analytical flow cytometry using a sample of each grouping. The remaining sorted 2° SVF cells from the original cohorts were loaded onto freshly prepared HFIP silk scaffolds by repeating the same process above. After incubation, the scaffolds were loaded with the 2° SVF cells and were implanted bilaterally into C57Bl/6 mice for a 6-week period. At that time, the scaffold harvest and analysis was repeated to yield a 3° SVF cell population. Due to cell harvest constraints, the scaffold harvest and analysis was terminated following 3° SVF cell populations, and 2 ° ASC populations. As a positive control, intact inguinal depots from C57Bl/6 (UBC-GFP) mice were serially transplanted to congenic wild type recipients for equivalent periods of time. Additionally, insulin sensitivity within the removed silk scaffold constructs was determined using our published *in vitro* glucose uptake and lipolysis assays to insure functionality[34]. It should be noted that for the present study time of engraftment was measured between the date of surgical implantation of the scaffold (with or without cells) and the date when it was surgically removed from the animal. For negative control groups, tissue was harvested from age and gender compatible non-GFP-Tg C57BL6 mice.

Hemoglobin saturation measurement

The Zenascope PC1 spectrometer employs a broadband halogen light source (probe) to illuminate the target tissue. The Zenascope allows measurements of protein levels in live animals, in the absence of invasive techniques. A bifurcated fiber optic probe with stainless steel jacketing and terminating in a 0.25” diameter stainless steel rigid common end is applied to the surface of the tissue, delivers light to the target tissue and collects the reflected optical signal, and the optical properties (wavelength-dependent absorption and scattering coefficients) of the tissue are quantitatively extracted from the measured reflectance spectra over the wavelength range 500–650 nm. From the extracted absorption coefficient, the portable and standardized measurement hardware achieves rapid, real-time quantitative analysis of oxyhemoglobin (HbO_2), deoxyhemoglobin (dHb), total hemoglobin concentration (Hb, defined as HbO_2 + dHb), and hemoglobin oxygen saturation (sO_2, defined as the ratio HbO_2/Hb). The optical reduced scattering coefficient (μ_s') was also measured and reported by the instrument, which allows measurements of tissue

chromophores to be quantified accurately and independently of changes in tissue scattering. Integration times were automatically set by the system software for each measurement to maximize reflectance signal while staying within the linear response range of the detector, and typically ranged from 100–200 ms. Reflectance calibration of the probe using a 99% reflectance standard was performed prior to all experiments and periodically during the procedures.

ImageJ Explant Analyses

For reporting on ASC or SVF enhancement engraftment time, 3 representative images of whole explants that were removed from each cohort were converted to TIF files and exported to Image J for analyses. Images from unseeded scaffold explants (control) were quantified using (ImageJ Version 1.46 software, NIH). Pixel values were from the entire tissue explant, not sectioned images. Threshold values were established from subtracting background pixel count using the control. Relative mean pixel counts from groups of tissue sections were averaged and the standard deviation was calculated.

Cryo-Scanning Electron Microscopy

Cryo-scanning electron microscopy was conducted on scaffolds that were seeded with GFP-Tg ASC following 24 h cell culture. Cryo-SEM structure research was done with Gatan 2500 alto Cryo-system and Hitachi S-4800 SEM. The tissue was cut to 7×5x5 (mm) and laid about 5mm high above a cryogenic SEM sample holder surface, clamped and glued into the holder, and then frozen in slushed liquid nitrogen at approximately −210°C for about 30 seconds. The frozen tissue was transferred in vacuum to the pre-chamber attached to the SEM and then fractured and sublimed for 5 minutes at −95°C. After coating 88 seconds at −130°C with Pt/Pd, the sample was moved to the SEM and observed at 3kV at −130°C.

Histochemistry

Fresh frozen tissue samples were sectioned, stained with a lipophilic fluorescent dye (Bodipy), and evaluated by confocal fluorescent microscopy for the co-localization of GFP and lipid signals.

qPCR for GFP gene expression

Total DNA was isolated from removed tissue engineered fat pads or positive or negative controls using the Qiagen FFPE tissue prep Mini Kit (Qiagen Inc. Valencia, CA, http://www.qiagen.com) according to the manufacturer's specifications. Polymerase chain reactions were performed with approximately 500 ng of total DNA using the SYBR green real-time PCR DNA binding dye. Reaction mix was incubated with Oligonucleotide primer sets specific for green fluorescent protein (GFP; forward: 5'-TCGCCTACCAGCTCATGCATAACA-3'; reverse: 5'-TGAAGCTCTTCCAGGTGTCAACGA-3') in a real-time thermal detection system (Bio-Rad Laboratories, Hercules, CA). All results were normalized relative to GAPDH expression control.

Statistics

All studies were repeated at least in triplicate and values are reported as the mean ± standard deviation (S.D.). Individual pairs were compared using the student T test while larger groups were analyzed by Analysis of Variance (ANOVA). Findings were defined as significant with minimum $P\ values \leq 0.05$.

Results

Isolation and characterization of cells utilized

Figure 1a provides the representative subpopulations of cells detected within GFP-SVF of iWAT isolated from 8–12 week male mice. Initial SVF yields averaged 3–5 × 10^5 1° (primary) SVF cells per ml of adipose tissue. This is similar to reported values in the literature[33]. The three largest subpopulations based on surface immunophenotype (Supplementary Table) were the pre-adipocytes, (24.7 ± 6.9%; $CD14^-$, $CD36^+$), the ASC-like (20 ± 10.7%; $CD146^-$, $CD34^+$, $CD90^+$), and the leukocytes (19.4 ± 9.7%; $CD34^-$, $CD45^+$). Of note, the pelleted SVF cell population excludes floating mature adipocytes (estimated to be about 30% of the total population) due to the process of collagenase type I tissue digestion and isolation by differential centrifugation. The initial SVF fraction was first sorted for the $CD146^-$ subpopulation (80.5 ± 5%). This served as the initial cohort of fractionated SVF cells. Other cohorts were selected based on sorting for CD34 and CD29 surface antigen expression: (b) $CD29^+$ (18.2 ± 8.5% of the CD146- population) and (c) $CD34^+$ (21.4 ± 12.8% of the CD146- population) SVF cells. The flow cytometry sorting protocol is given in Figure 2. Characteristics of these cohorts ((a) total $CD146^-$ SVF cells, (b) $CD146^-$, $CD29^+$ enriched cells, and (c) $CD146^-$, $CD34^+$ enriched cells) were determined based on immunophenotype of plastic adherent cell culture, proliferation, colony formation, and adipogenic potential out to passage 2 (P2). Similar to other published reports, stromal markers (CD29) increased in expression, and endothelial (CD31, CD45) and hematopoietic markers (CD34, CD11b) decreased in expression over passage. Sca-1 expression averaged 61.6 ± 10.7% within unsorted SVF populations and increased over passage (Figure 2a). CD29 and CD34 enrichment resulted in lower Sca-1 expression (CD29; 13.8 ± 2.4%, CD34, 13.7 ± 0.9%). $CD34^+$ enriched subpopulations exhibited significantly higher proliferative and adipogenic potential than $CD29^+$ enriched subpopulations (Figure 2b). Further, $CD29^+$ subpopulations had slower doubling times and lower intra-cytoplasmic lipid accumulation than the unsorted populations (Figure 2c, 2d).

SVF and ASC seeding on scaffolds

GFP-ASC *In vitro* seeding and proliferative properties were investigated following seeding on HFIP-based silk scaffolds. Confocal microscopy was performed on seeded and unseeded control scaffolds after 24 hours of incubation (Supplementary Figure 2a). GFP detection and Alamar Blue staining revealed a preference of cell localization on the edges of the silk scaffold honeycomb-like structures (Supplementary Figure 2b, bright field, and 2d, scanning electron microscopy). Cells remained on these edges, commenced differentiation (Supplementary Figure 2c) and proliferation (Supplementary Figure 2d, and Figure S2e). Quantitation of Alamar Blue (Supplementary Figure 2d) cytosolic and DAPI (Supplementary Figure 2e) nuclear positivity revealed the cells were present 2 hours post

seeding (18 hr.; 16 ± 2 cells; 2hr., 11 ± 8 cells; Supplementary Figure 2e), but adhered to the scaffold and exhibited measurable metabolic activity by relative fluorescence intensity 18 hours post seeding (18 hr., 36 RFU; 2hr., 0.001 RFU; Supplementary Figure 2e).

SVF cells enhance engraftment and generate adipose in vivo

Unfractionated SVF cells were monitored for growth and adipogenesis using a 6-week time course. Photographic analyses revealed that the presence of SVF cells accelerated engraftment by week 1(Figure 3a). Measurements of percent hemoglobin saturation (% Hb; Figure 3b) also supported the observed SVF cell-mediated enhanced vascularization. It should be noted that hemoglobin measurements were taken on the skin surface of live mice, and that the measurement of saturation assesses all tissues, not simply the arterial blood supply. By week 2 and beyond, no significant difference in engraftment was observed, both visually and by quantification of explant images using ImageJ (Figure 3c). This supported published data suggesting the vascular and supportive nature of the scaffolds to promote adipogenesis *in vivo*. Measurements of scaffold mass (Figure 3d) and total SVF recovered (Figure 3e) from seeded scaffolds were significantly higher than unseeded controls during week 1. SVF cell count and scaffold mass reached a maximum at week 2, and decreased by week 4 (Panels 3d–e).

Unsorted GFP-SVF cells detected following serial transplantation

Weekly detection of unsorted GFP-SVF within initial implants from weeks one to six (Figure 4a) revealed that GFP-SVF cells were not only persisting within scaffolds, but also proliferating and differentiating as early as week 1 following implantation. Confocal microscopy images are displayed for weeks 1, 4, 5, and 6 of initial SVF explants (Figure 4a). GFP-Tg SVF cells were detected within explants from initial cohorts (T_0 implants), as well as initial serial (T_1 implants) and secondary serial (T_2 implants; Figure 4b) transplants. Flow cytometry based detection of GFP-Tg SVF cells was consistent with confocal microscopy observations (Figure 4c). Initial implants resulted in 19% GFP antigen positivity via flow cytometry at week 4 while T_1 and T_2 implants resulted in 16.2% and 13.1% GFP positivity, respectively, at the same time points relative to implantation (Figure 4c). Quantification of GFP, BODIPY lipophilic dye staining (to demonstrate the adipogenic nature of the constructs), and the nuclear DAPI stain co-localization was performed using ImageJ. Quantification demonstrated a 50% increase in GFP-Tg SVF cell percentage by week 6 following T_0 implants, compared to week 1 (Figure 4d). It is important to note that the flow cytometry data reported in figure 4d is conducted on the SVF cells that have been isolated from the tissue reported in figure 4c. Adipose tissue contains mature adipocytes and other cells that would not survive the tissue digestion procedure, and would not be reflected in the flow cytometry numbers. Figure 4d therefore does not reflect all cells in the tissue sample. GFP expression within removed explants was further investigated based on protein and DNA levels via flow cytometry and qPCR, respectively (Figure 4e, f). Weekly detection of percent GFP-Tg cells via flow cytometry revealed an increase in expression from 3.8% in week 2 to 16% by week 4 following T_0 implants (Figure 4e). GFP DNA expression was enriched more than 200 fold (unseeded scaffold implants in non-transgenic mice) following T_2 implants (Figure 4f). The surface immunophenotype of cells from the T_2 implant population was also compared to GFP-Tg controls and unseeded scaffold controls following 6 weeks (Figure 4g).

The T_2 scaffolds displayed 36.3 ± 2.4% GFP positivity, 67.8 ± 4.1%CD29 positivity, and 52.4 ± 2.4% CD45 positivity (Figure 4g).

CD34-enriched *GFP-Tg* ASC enhance engraftment and generate functional adipose in vivo

GFP-Tg SVF cells were isolated and grouped as unfractionated cells, or sorted as $CD146^-$ $CD29^+$ enriched, or $CD146^-$ $CD34^+$ enriched groupings. These cells were culture expanded to P2 GFP-Tg ASC, seeded on silk scaffolds, and implanted into non-transgenic mice until T_0 serial transplant. No visual difference in fat depot size was observed at week 6 of implant removal (Figure 5a, b). Measurements of percent hemoglobin (%Hb) saturation and explant engraftment were investigated. Implants seeded with both CD29- and CD34-enriched GFP-Tg ASC exhibited higher %Hb saturation following 1 week of implantation compared to both unseeded implants and implants seeded with unsorted ASC control (Figure 5c). Further, CD34-enriched implants exhibited significantly higher %Hb saturation than CD29-enriched implants (Unseeded ASC: control, 37.6 ± 9.9%; CD34-enriched, 68.1 ± 5.3%; CD29-enriched, 45 ± 10.8%; Figure 5c). This was observed visually and quantitatively using ImageJ software analyses of photomicrographs (Figure 5d). Measurements of explant mass and mass of the surrounding fat (Figure 5e) revealed that the engineered constructs originating from CD34-enriched implants were significantly more dense than CD29-enriched and unsorted GFP-Tg ASC, as well as unseeded controls (5e). Total SVF recovered (Figure 5f) from CD34-enriched ASC seeded scaffolds were also significantly higher than CD29-enriched, unsorted ASC, and unseeded controls during week 1 (Figure 5f). Further investigation of tissue engineered fat functionality revealed CD34-enriched constructs secreted glycerol levels comparable to unsorted ASC constructs, whereas CD29-enriched constructs secreted significantly lower levels of glycerol (Figure 5g). No significant difference was observed in glucose uptake between cohorts (Figure 5h).

$CD146^-$ $CD34^+$/$CD29^+$ GFP-Tg ASC detected following serial transplantation

GFP-Tg ASC were detected within 6-week explants from initial cohorts (T_0 implants), as well as initial serial (T_1 implants; Figure 6a). Tissue implants were infiltrated with blood vessels, which supports the earlier observation of tissue engraftment with GFP-Tg SVF and GFP-Tg ASC seeded scaffolds. Flow cytometry based detection of freshly isolated GFP-Tg cells supported confocal microscopy observations of GFP positivity following week 6 of implantation (Figure 6c–d). Initial CD34-enriched constructs resulted in detection of 29.4% GFP antigen positivity, compared to CD29-enriched constructs, which resulted in 10.9% GFP positivity via flow cytometry (Figure 6c). CD34-enriched and CD29-enriched T_1 implants resulted in 20.4% and 8.4% GFP positivity, respectively (Figure 6d). Quantification of GFP, BODIPY lipophilic dye, and DAPI co-localization staining was performed using ImageJ. GFP expression within explants was further investigated based on DNA and protein levels via qPCR and flow cytometry, respectively (Figure 6e, f–g). GFP DNA detected was 15-fold higher in CD34-enriched constructs compared to CD29-enriched constructs, and more than 10-fold higher than unsorted ASC constructs following T_1 implants (Figure 6e). Detection of percent GFP-Tg cells via flow cytometry supported a significant difference in expression of GFP-Tg cells from CD34-enriched constructs compared to CD29-enriched constructs following 8 week T_0 implants (CD29, 9.8 ± 1.1; CD34, 24.7 ± 6.5; Figure 6f) and T_1 implants (CD29, 5.4 ± 1.2; CD34, 17.5 ± 1.4; Figure 6g).

CD146^{-} CD34^{+}-enriched constructs generate functional GFP^{+} fat in vivo

Adipose surrounding removed 8 week serial implants from GFP-Tg SVF seeded, unsorted GFP-Tg ASC, GFP-Tg CD34-enriched ASC, GFP-Tg CD29-enriched ASC, and GFP positive and negative controls, were removed and analyzed for GFP positivity (Figure 7a–c) and functionality (Figure 7d, e). Confocal microscopy images of BODIPY stained removed adipose surrounding 8-week constructs revealed a significant increase in percent GFP-Tg adipocytes in CD34-enriched cohorts compared to CD29-enriched, unsorted ASC, and SVF-seeded constructs (Figures 7a, b). Quantification of images using ImageJ supported visual observations (SVF, 2.5 ± 1.7%; unsorted GFP-Tg ASC, 15.5 ± 0.2%; CD29-enriched, 6.1 ± 7.0%; CD34-enriched, 31.3 ± 0.4%; Figure 7c). Further investigation of tissue engineered fat functionality revealed CD34-enriched constructs secreted glycerol levels comparable to unsorted ASC constructs whereas CD29-enriched constructs secreted significantly lower levels of glycerol (CD34, 70 ± 16.1μM; unsorted ASC, 75 ± 22.1μM; CD29, 40 ± 14.6 μM; Figure 7d). Similar to removed constructs in Figure 5, no significant difference was observed in glucose uptake between cohorts (Figure 7e).

Discussion

The present study transplanted freshly isolated GFP-Tg SVF cells using 3-D silk matrices into non-GFP-Tg transgenic syngeneic murine hosts successfully over one initial, and two serial implants (2° implants). Initial time-based implant removal studies demonstrated GFP-Tg SVF cell survival, proliferation, and differentiation, leading to the formation of metabolically functional adipose tissue. Time-based GFP-Tg SVF experiments also revealed SVF cell ability to enhance engraftment and to reduce engraftment time. Expanded, plastic-adherent CD146^{-} CD29^{+} and CD146^{-} CD34^{+} P2 GFP-Tg ASC populations were seeded on 3-D matrices, and implanted into non-GFP-Tg transgenic hosts successfully for an initial and serial implant (1° implants). To our knowledge, we are among the first to report the ability of specific subpopulations of non-pericytic ASC within the stromal vascular compartment to generate functional adipose over serial transplants.

These experiments were modeled after the serial transplant studies in the bone marrow literature which first validated the existence of HSCs[1]. The studies by Till, McCulloch and others demonstrated that when hematopoietic cells were removed from the bone marrow and re-injected into γ-irradiated syngeneic recipient hosts, they would repopulate the bone marrow and restore basal hematopoietic activity[1, 36]. The present study supports the current literature suggesting that SVF cells and ASC have the ability to generate functional adipose tissues, and extends those observations to serial implantation of CD146^{-} CD34^{+}-enriched GFP-Tg ASC, similar to the well-established HSC model [1, 34, 36–39]. Mauney, et. al. reported on the ability of ASC to generate fat pads in rats using engineered scaffolds[34]. The objectives of their study included comparing biomaterials derived from silk fibroin prepared by aqueous (AB) and organic (HFIP) solvent-based processes, along with collagen and poly-lactic acid (PLA)-based scaffolds, for their utility in adipose tissue engineering strategies. Their findings revealed HFIP silk based matrices were superior to the other biomaterials and therefore suitable for other applications such as the current study. The current study therefore confirms and extends the findings by Mauney, et. al; however, the novelty is

application of a more heterogeneous stromal vascular population, and usage in serial transplantation.

Due to the limitations of mouse tissue volume, ASC used in the present study were pooled from multiple mouse donors, and starting sample sizes for serial transplants were n=20. A caveat within the current study is the usage of CD34 enriched and CD29 enriched ASC populations that were expanded from freshly isolated mouse GFP-SVF; not CD34-exclusive and CD29-exclusive populations. Due to the rarity of $CD29^+/CD34^+$ double positive and $CD29^-/CD34^-$ double negative subpopulations within the freshly isolated SVF subfraction, the groupings in the current study contained culture-expanded $CD34^+$ cells without consideration of CD29 co-expression. The same selection was used for CD29, without consideration of CD34 co-expression. Therefore, a subpopulation within the $CD34^+$ GFP-ASC population also co-expressed CD29 and other cell surface and intracellular stromal markers that may be involved in anchorage, proliferation, migration, and adipogenic regulation. $CD34^+$ populations within freshly isolated murine SVF cells averaged 21.4% in the unsorted population; however, the $CD34^+$-enriched population in the SVF maintained an average of 33% positivity after 2 passages in culture. The percentage $CD34^+$ GFP-Tg ASC in this study are similar to published reports on CD34 positivity within human SVF[38]. The human CD34 positive populations were demonstrated to possess enhanced proliferative and adipogenic potential *in vitro*. A strong correlation was also identified between $CD34^+$ ASC yield and xenograft adipose tissue volume retention, suggesting that concentration of the $CD34^+$ progenitor can predict human fat graft survival in clinical settings[38]– [41]. Future experiments will extend the study to a more humanized system, initially by examining the behavior of sorted human cells in an immunodeficient murine model. These experiments will also allow for larger initial sample sizes that are greater than n=20, and may lead to serial transplantation beyond secondary transplants (3° and beyond).

The current literature refers to cells that aid in fat grafting survival using the terms, ‘adipose stromal’ cell and ‘perivascular stem’ cell interchangeably. Traditionally, perivascular stem cells are identified based on an immunophenotype of $CD45^-$, $CD146^+$, and $CD34^-$ [41]. The results from $CD146^-$ $CD34^+$-enriched ASC serial implants indicate the presence of a non-pericytic ASC subpopulation within SVF that is capable of generating functional fat pads in mice over successive transplants. These findings are supported by *in* vivo cell fate/mapping studies where tissue resident stem cells in neonatal mice were labeled with bromo-deoxyuridine (BrdU) [43]. Eight weeks later, histological analyses of inguinal adipose depots determined that the BrdU label retaining stem cells could be found in the perivascular space (consistent with a pericytic subpopulation) and at a substantial distance from the capillaries, in the vicinity of mature adipocytes (consistent with a non-pericytic population) [43]. Although the $CD146^-$ population represents the majority of the plastic-adherent population (80%) in the current study, only 20% of these cells co-express the progenitor cell antigen CD34. Nevertheless, the current results indicate that non-pericytic cells can serve as adipogenic stem cells in vivo.

Confocal fluorescence imaging measurements of %Hb saturation at weeks 1 and 4 demonstrated that the presence of GFP-Tg SVF or enriched GFP-Tg ASC accelerated scaffold engraftment as early as week 1 of implantation. Measurements of the SVF

recovered from the explants and scaffold weights at weeks 1 and 2 supported these data. Current published reports suggest SVF and ASC encourage the enhancement of engraftment and acceleration of wound healing in a variety of applications, including both soft and hard tissue remodeling, and for the improvement of pathophysiological conditions[44]. Mesimaki, et. al. demonstrated the usage of expanded ASC for the enhancement of a maxillary flap with beta-tricalcium phosphate and bone morphogenetic protein 2 (BMP2). Addition of the expanded ASC aided in the development of mature bone structures and vasculature[45]. Yoshimura, et. al. reported high surgeon and patient satisfaction 12 months postoperatively in 55 patients receiving adipose tissue grafts augmented with SVF cells, a procedure termed "cell-assisted lipotransfer (CAL)", instead of prosthetic breast enhancement[46]. More recently, Bura et al. have employed autologous human ASC to treat patients with critical ischemic limbs and have observed significant improvements in tissue oxygen delivery[47]. Together, these human clinical studies lend credence to the findings in our murine pre-clinical model.

Confocal microscopy and flow cytometric analyses of 8-week serial implants indicated that $CD34^+$ -enriched subpopulations are capable of generating functional fat pads, similar to unsorted ASC implants. $CD34^+$-enriched ASC were demonstrated to proliferate and undergo adipogenic differentiation at higher rates than $CD29^+$-enriched and unsorted ASC *in vitro*. *In vivo*, higher percentages of SVF cells were recovered from CD34-enriched constructs. These explants averaged higher scaffold masses than CD29-enriched and unsorted ASC cohorts. Functional analyses of fat surrounding the scaffolds after 6 weeks revealed CD34-enriched explants exhibited higher glycerol secretion than CD29-enriched, unsorted ASC, and control unseeded implants. GFP-Tg SVF and –ASC were detected within surrounding adipose depots. BODIPY staining, glycerol uptake, and lipolysis analyses suggest these cells may have been proliferating, differentiating within the scaffold, and migrating locally as mature adipocytes or as preadipocytes. These data suggest that a subpopulation phenotypically found within the $CD146^-$ $CD34^+$-enriched ASC population is capable of generating functional fat pads over serial passages. These findings are consistent with studies by Philips et al. demonstrating that the functionality and volume retention of human adipose tissue xenografts correlated with the frequency of $CD34^+$ cells in the donor tissue[38].

It remains challenging to distinguish cell categories between "stromal/progenitor" and "stem" cell. Nevertheless, the current serial transplant findings suggest that the inguinal WAT of adult mice contains a flow cytometry, sortable subpopulation of cells capable of contributing to the regeneration and serial transplantation of a functional adipose tissue depot. These findings confirm and extend earlier studies by Rodeheffer and others examining the ability of flow cytometry sorted adipose-derived cells to regenerate adipose depots in lipodystrophic mice [49–50]. Additionally, these outcomes further validate the utility of autologous adipose-derived cells for functional tissue engineering[51].

Supplementary Material

Refer to Web version on PubMed Central for supplementary material.

Acknowledgments

Acknowledgement and Disclosures

This work was funded in part by funding from the National Institutes of Health (R21DK094254). JMG is the co-owner, co-founder, and Chief Scientific Officer of LaCell LLC, a biotechnology company focusing research and clinical translation of adipose-derived stromal/stem cells.

JQB has financial interest and serves as a consultant for Zenalux Biomedical, Inc., a manufacturer of the quantitative tissue optical spectrometer used in this work.

References

1. Till JE, McCulloch EA, Siminovitch L. A Stochastic Model of Stem Cell Proliferation, Based on the Growth of Spleen Colony-Forming Cells. Proceedings of the National Academy of Sciences of the United States of America. 1964; 51:29–36. published online EpubJanVoss O, *et. al.*, 1972. [PubMed: 14104600]
2. Ramalho-Santos M, Willenbring H. On the origin of the term “stem cell”. Cell stem cell. 2007; 1:35–38. published online EpubJun 7(10.1016/j.stem.2007.05.013). [PubMed: 18371332]
3. Zuk PA, et al. Human Adipose Tissue is a Source of Multipotent Stem Cells. Mol Biol Cell. 2002 Dec; 13(12):4279–4295. [PubMed: 12475952]
4. Guilak F, Lott KE, Awad HA, et al. Clonal analysis of the differentiation potential of human adipose derived adult stem cells. J Cell Physiol. 2006; 206:229–237. [PubMed: 16021633]
5. Izadpanah R, Trygg C, Patel B, et al. Biologic properties of mesenchymal stem cells derived from bone marrow and adipose tissue. J Cell Biochem. 2006; 99:1285–1297. [PubMed: 16795045]
6. Maumus M, Peyrafitte JA, D’Angelo R, et al. Native human adipose stromal cells; localization, morphology, and phenotype. Int J Obesity (London). 2011; 9:1141–1153.
7. Kim JH, Jee MK, Lee SY, Han TH, Kim BS, Kang KS, Kang SK. Regulation of adipose tissue stromal cells behaviors by endogenic Oct4 expression control. Plos One. 2009 Sep 24.4(9):e7166. [PubMed: 19777066]
8. Crossno JT, Majka SM, Grazia T, Gill RG, Klemm DJ. Rosiglitazone promotes development of a novel adipocyte population from bone marrow-derived circulating progenitor cells. J Clin Inves. 2006 Dec; 116(12):3220–3228.
9. Koh YJ, Kang S, Lee HJ, Choi TS, Lee HS, Cho CH, Koh GY. Bone marrow-derived circulating progenitor cells fail to transdifferentiate into adipocytes in adult adipose tissues in mice. J Clin Inves. 2007 Dec; 117(12):3684–3695.
10. Majka SM, Fox KE, Psilas JC, Helm KM, Childs CR, Acosta AS, Janssen RC, Friedman JE, Woessner BT, Shade TR, Varella-Garcia M, Klemm DJ. De novo generation of white adipocytes from the myeloid lineage via mesenchymal intermediates is age, adipose depot, and gender specific. J Clin Inves. 2010 Aug 17; 107(33):14781–14786.
11. Zannetinno Paton S, Arthur A, Khor F, Itescu S, Gimble JM, Gronthos S. Multipotential human adipose-derived stromal stem cells exhibit a perivascular phenotype in vitro and in vivo. J Cell Physiol. 2008 Feb; 214(2):413–421. [PubMed: 17654479]
12. Crisan M, Yap S, Casteilla L, Chen CW, Corselli M, Park TS, Andriolo G, Sun B, Zheng B, Zhang L, Norotte C, Teng PN, Traas J, Schugar R, Deasy BM, Badylak S, Buhring HJ, Giacobino JP, Lazzari L, Huard J, Péault B. A perivascular origin for mesenchymal stem cells in multiple human organs. Cell Stem Cell. 2008 Sep 11; 3(3):301–313. [PubMed: 18786417]
13. Traktuev DO, Merfeld-Clauss S, Li J, Kolonin M, Arap W, Pasqualini R, Johnstone BH, March KL. A population of multipotent CD34-positive adipose stromal cells share pericyte and mesenchymal surface markers, reside in a periendothelial location, and stabilize endothelial networks. Circ Res. 2008 Jan 4; 102(1):77–85. [PubMed: 17967785]
14. Gimble JM, Katz AJ, Bunnell BA. Adipose-derived stem cells for regenerative medicine. Circ Res. 2007 May 11; 100(9):1249–1260. [PubMed: 17495232]

15. Yoshimura K, Sato K, Aoi N, Kurita M, Inoue K, Suga H, Eto H, Kato H, Hirohi T, Harii K. Cell-assisted lipotransfer for facial lipoatrophy: efficacy of clinical use of adipose-derived stem cells. Dermatol Res. 2009 Sep; 34(9):1178–1185.

16. Yoshimura K, Asano Y, Aoi N, Kurita M, Oshima Y, Sato K, Inoue K, Suga H, Eto H, Kato H, Harii K. Breast J. 2010 Mar-Apr;16(2):169–175. [PubMed: 19912236]

17. Rubin JP, Marra KG. Soft tissue reconstruction. Methods Mol Biol. 2011; 702:395–400. [PubMed: 21082417]

18. Maggini J, Mirkin G, Bognanni I, Holmberg J, Piazzón IM, Nepomnaschy I, Costa H, Cañones C, Raiden S, Vermeulen M, Geffner JR. Mouse bone marrow-derived mesenchymal stromal cells turn activated macrophages into a regulatory-like profile. Plos One. 2010 Feb 16.5(2):e9252. [PubMed: 20169081]

19. Al-Zoubin M, Salem AF, Martinez-Outschoorn UE, Whitaker-Menezes D, Lamb R, Hulit J, Howell A, Gandara R, Sartini M, Arafat H, Bevilacqua G, Sotgia F, Lisanti MP. Creating a tumor-resistant microenvironment: cell-mediated delivery of TNFα completely prevents breast cancer tumor formation in vivo. Cell Cycle. 2013 Feb 1; 12(3):480–490. [PubMed: 23292149]

20. Li P, Sun H, Du M, Fa Z, Qin K, Xu W, Zhang R, Chen L, Yao C, Xiao Z, Zhang S, Ke Y, Jiang X. Adult rat hippocampus soluble factors: a novel transplantation model mimicking intracranial microenvironment for tracing the induction and differentiation of adipose-derived stromal cells in vitro. Neurosci Lett. 2013 May 10.542:5–11. [PubMed: 23103714]

21. Mazo M, Planat-Bénard V, Abizanda G, Pelacho B, Léobon B, Gavira JJ, Peñuelas I, Cemborain A, Pénicaud L, Laharrague P, Joffre C, Boisson M, Ecay M, Collantes M, Barba J, Casteilla L, Prósper F. Transplantation of adipose derived stromal cells is associated with functional improvement in a rat model of chronic myocardial infarction. Eur J Heart Fail. 2008 May; 10(5): 454–462. [PubMed: 18436478]

22. Cai L, Johnstone BH, Cook TG, Tan J, Fishbein MC, Chen PS, March KL. IFATS collection: Human adipose tissue-derived stem cells induce angiogenesis and nerve sprouting following myocardial infarction, in conjunction with potent preservation of cardiac function. Stem Cells. 2009 Jan; 27(1):230–237. [PubMed: 18772313] Schenke-Layland K, MacLellan WR. Induced pluripotent stem cells: it's like déjà vu all over again. Circulation. 2009 Oct 13; 120(15):1462–1464. [PubMed: 19786628]

23. Kang SK, Lee S, Oh HK, Kang MW, Na MH, Yu JH, Koo BS, Lim SP. Clinical features of deep neck infections and predisposing factors for mediastinal extension. Korean J Thorac Cardiovasc Surg. 2012 Jun; 45(3):171–176. [PubMed: 22708085]

24. Kim JM, Lee ST, Chu K, Jung KH, Song EC, Kim SJ, Sinn DI, Kim JH, Park DK, Kang KM, Hyung Hong N, Park HK, Won CH, Kim KH, Kim M, Kun Lee S, Roh JK. Systemic transplantation of human adipose stem cells attenuated cerebral inflammation and degeneration in a hemorrhagic stroke model. Brain Res. 2007 Dec 5.1183:43–50. [PubMed: 17920570]

25. Ikegame Y, Yamashita K, Hayashi S, Mizuno H, Tawada M, You F, Yamada K, Tanaka Y, Egashira Y, Nakashima S, Yoshimura S, Iwama T. Comparison of mesenchymal stem cells from adipose tissue and bone marrow for ischemic stroke therapy. Cytotherapy. 2011 Jul; 13(6):675–685. [PubMed: 21231804]

26. Rehman J, Traktuev D, Li J, Merfeld-Clauss S, Temm-Grove CJ, Bovenkerk JE, Pell CL, Johnstone BH, Considine RV, March KL. Secretion of angiogenic and antiapoptotic factors by human adipose stromal cells. Circulation. 2004 Mar 16; 109(10):1292–1298. [PubMed: 14993122]

27. Planat-Benard V, Silvestre JS, Cousin B, André M, Nibbelink M, Tamarat R, Clergue M, Manneville C, Saillan-Barreau C, Duriez M, Tedgui A, Levy B, Pénicaud L, Casteilla L. Plasticity of human adipose lineage cells toward endothelial cells: physiological and therapeutic perspectives. Circulation. 2004 Feb 10; 109(5):656–663. [PubMed: 14734516]

28. Moon MH, Kim SY, Kim YJ, Kim SJ, Lee JB, Bae YC, Sung SM, Jung JS. Human adipose tissue-derived mesenchymal stem cells improve postnatal neovascularization in a mouse model of hindlimb ischemia. Cell Physiol Biochem. 2006; 17(5–6):279–290. [PubMed: 16791003]

29. Bura A, Planat-Benard V, Bourin P, Silvestre JS, Gross F, Grolleau JL, Saint-Lebese B, Peyrafitte JA, Fleury S, Gadelorge M, Taurand M, Dupuis-Coronas S, Leobon B, Casteilla L. Phase I trial: the use of autologous cultured adipose-derived stromal/stem cells to treat patients with non-

revascularizable critical limb ischemia. Cytotherapy. 2014; 16:245–257. published online EpubFeb (10.1016/j.jcyt.2013.11.011). [PubMed: 24438903]

30. Yu G, Wu X, Kilroy G, et al. Isolation of murine adipose-derived stem cells. Methods Mol Biol. 2011; 702:29–36. [PubMed: 21082392]
31. Mitchell JBMK, Zvonic S, Garrett S, Floyd ZE, Kloster A, Halvorsen YD, Storms RW, Goh B, Kilroy GS, Wu X, Gimble JM. The immunophenotype of human adipose derived cells: Temporal changes in stromal- and stem cell-associated markers. Stem Cells. 2006; 24:376–385. [PubMed: 16322640]
32. Crisan M, Yap S, Casteilla L, Chen C-W, Corselli M, et al. A Perivascular Origin for Mesenchymal Stem Cells in Multiple Human Organs. Cell Stem Cell. 2008; 3:301–313. [PubMed: 18786417]
33. Zimmerlin L, Donnenberg VS, Rubin JP, Donnenberg AD. Mesenchymal markers on human adipose stem/progenitor cells. Cytometry. Part A : the journal of the International Society for Analytical Cytology. 2013; 83:134–140. published online EpubJan (10.1002/cyto.a.22227). [PubMed: 23184564]
34. Mauney JR, Nguyen T, Gillen K, Kirker-Head C, Gimble JM, Kaplan DL. Engineering Adipose-like Tissue in vitro and in vivo Utilizing Human Bone Marrow and Adipose-derived Mesenchymal Stem Cells with Silk Fibroin 3D Scaffolds. Biomaterials. 2007; 28:5280–5290. [PubMed: 17765303]
35. Hebert TL, Wu X, Yu G, et al. Culture effects of epidermal growth factor (EGF) and basic fibroblast growth factor (bFGF) on cryopreserved human adipose-derived stromal/stem cell proliferation and adipogenesis. J Tissue Eng Regen Med. 2009; 3:553–561. [PubMed: 19670348]
36. Vos O, Dolmans MJ. Self-renewal of colony forming units (CFU) in serial bone marrow transplantation experiments.
37. Barnes DW, Ford CE, Loutit JF. Serial grafts of homologous bone marrow in irradiated mice. Sang. 1959; 30:762–765. [PubMed: 13796874]
38. Philips BJ, Grahovac TL, Valentin JE, Chung CW, Bliley JM, Pfeifer ME, Roy SB, Dreifuss S, Kelmendi-Doko A, Kling RE, Ravuri SK, Marra KG, Donnenberg VS, Donnenberg AD, Rubin JP. Prevalence of endogenous CD34+ adipose stem cells predicts human fat graft retention in a xenograft model. Plastic and reconstructive surgery. 2013; 132:845–858. published online EpubOct (10.1097/PRS.0b013e31829fe5b1). [PubMed: 23783061]
39. Yoshimura K, Eto H, Kato H, Doi K, Aoi N. In vivo manipulation of stem cells for adipose tissue repair/reconstruction. Regenerative medicine. 2011; 6:33–41. published online EpubNov (10.2217/rme.11.62). [PubMed: 21999260]
40. Yoshimura K, Sato K, Aoi N, Kurita M, Hirohi T, Harii K. Cell-assisted lipotransfer for cosmetic breast augmentation: supportive use of adipose-derived stem/stromal cells. Aesthetic plastic surgery. 2008; 32:48–55. discussion 56-47 published online EpubJan (10.1007/s00266-007-9019-4). [PubMed: 17763894]
41. Li H, Zimmerlin L, Marra KG, Donnenberg VS, Donnenberg AD, Rubin JP. Adipogenic potential of adipose stem cell sub- populations. Plast Reconstr Surg. 2011; 128:663–672. [PubMed: 21572381]
42. James AW, Zara JN, Corselli M, Askarinam A, Zhou AM, et al. An abundant perivascular source of stem cells for bone tissue engineering. Stem Cells Transl Med. 2012:673–684. [PubMed: 23197874]
43. Gawronska-Kozak B, Staszkiewicz J, Gimble JM, Kirk-Ballard H. Recruitment of fat cell precursors during high fat diet in C57BL/6J mice is fat depot specific. Obesity. 2014; 22:1091–1102. published online EpubApr (10.1002/oby.20671). [PubMed: 24795999]
44. Kokai LE, Marra K, Rubin JP. Adipose stem cells: biology and clinical applications for tissue repair and regeneration. Translational Research. 2014; 163:399–408. [PubMed: 24361334]
45. Mesimaki K, Lindroos B, Tornwall J, et al. Novel maxillary reconstruction with ectopic bone formation by GMP adipose stem cells. Int J Oral Maxillofac Surg. 2009; 38:201–209. [PubMed: 19168327]
46. Yoshimura K, Asano Y, Aoi N, et al. Cell-assisted lipotransfer for cosmetic breast augmentation: supportive use of adipose-derived stem/stromal cells. Aesthet Plast Surg. 2008; 32:48–57.

47. Bura A, Planat-Benard V, Bourin P, Silvestre JS, Gross F, Grolleau JL, Saint-Lebese B, Peyrafitte JA, Fleury S, Gadelorge M, Taurand M, Dupuis-Coronas S, Leobon B, Casteilla L. Phase I trial: the use of autologous cultured adipose-derived stroma/stem cells to treat patients with non-revascularizable critical limb ischemia. Cytotherapy. 2014; 16:245–257. published online EpubFeb (10.1016/j.jcyt.2013.11.011). [PubMed: 24438903]

48. Berry R, Rodeheffer MS. Characterization of the adipocyte cellular lineage in vivo. Nature cell biology. 2013; 15:302–308. published online EpubMar (10.1038/ncb2696). [PubMed: 23434825]

49. Rodeheffer MS, Birsoy K, Friedman JM. Identification of white adipocyte progenitor cells in vivo. Cell. 2008; 135:240–249. published online EpubOct 17 (10.1016/j.cell.2008.09.036). [PubMed: 18835024]

50. Ramalho-Santos M, Willenbring H. On the origin of the term “stem cell”. Cell stem cell. 2007; 1:35–38. published online EpubJun 7 (10.1016/j.stem.2007.05.013). [PubMed: 18371332]

51. Hu L, Yang G, Hägg D, Sun G, Ahn JM, Jiang N, Ricupero CL, Wu J, Rodhe CH, Ascherman JA, Chen L, Mao JJ. IGF1 Promotes Adipogenesis by a Lineage Bias of Endogenous Adipose Stem/Progenitor Cells. Stem Cells. 2015; 33(8):2483–2495. [PubMed: 26010009]

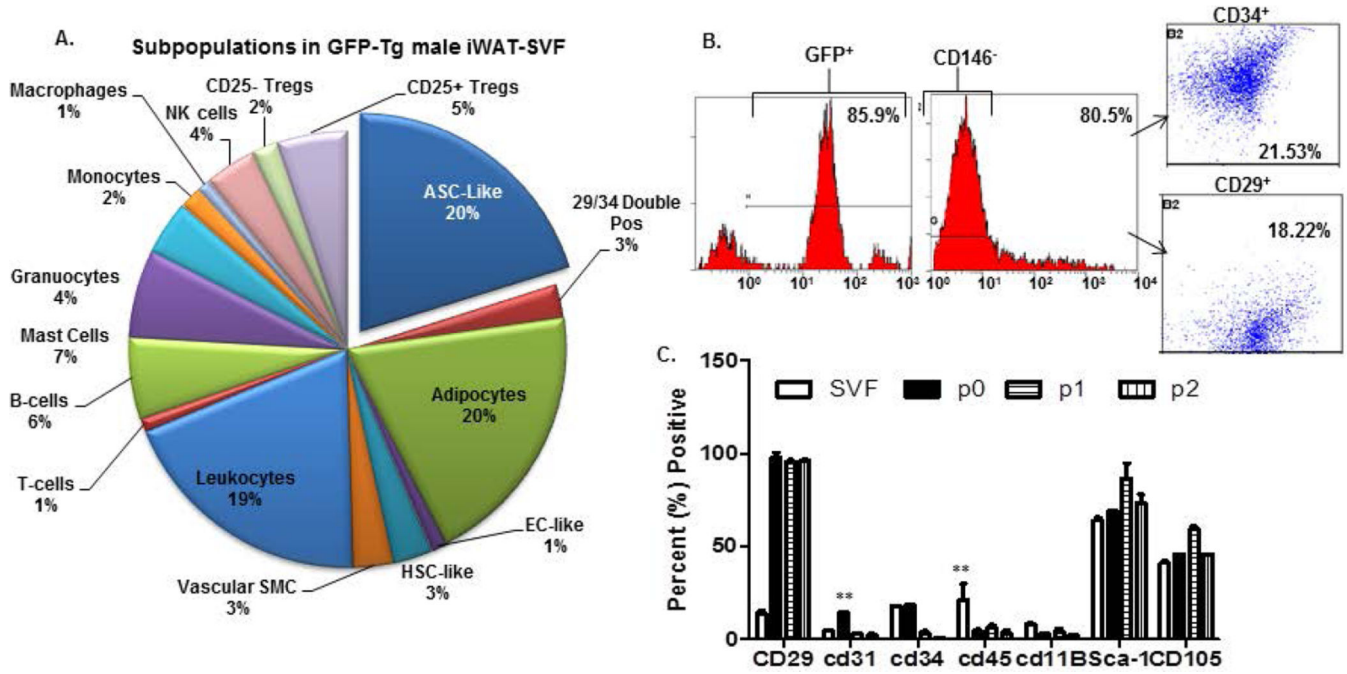

Figure 1. Characterization of cells used in the study

1a). Pie chart of subpopulations within GFP-Tg SVF cells that were utilized for SVF serial transplantation studies. 1b). Sorting and enrichment of $CD146^{-}$ $CD29^{+}$, and $CD146^{-}$ $CD34^{+}$ subpopulations that were culture expanded to P2 ASC for GFP-Tg ASC serial transplantation studies. 1c). Immunophenotype of GFP-Tg SVF cells and culture-expanded GFP-Tg ASC, until passage 2 (P2). All experiments were repeated in triplicate; sample size, n=3 per replicate. Values reported as mean ± standard deviation (μ ± SD); *$p < 0.05$, ** $p < 0.01$; ***$p < 0.001$.

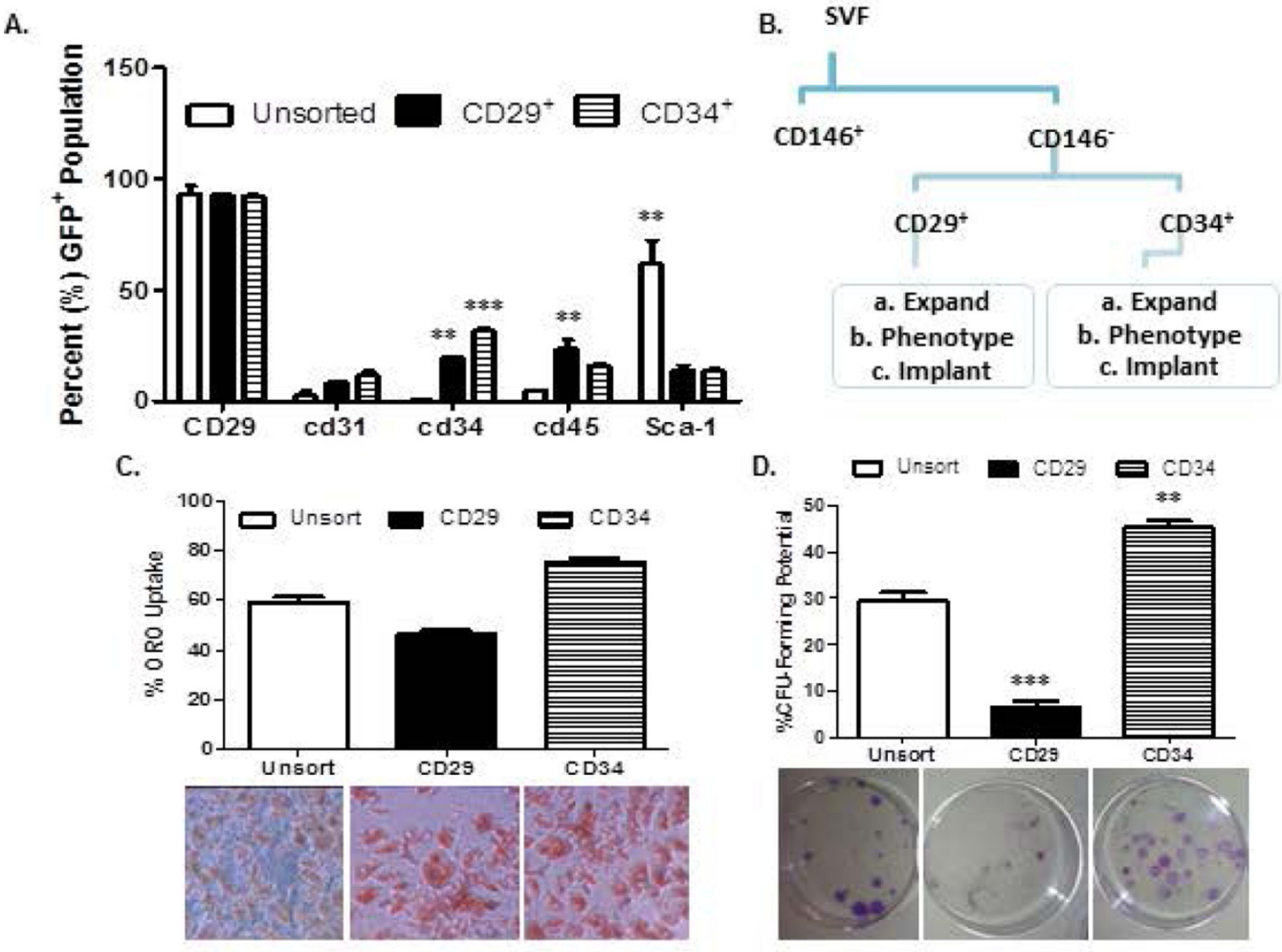

Figure 2. Comparison of CD29-enriched and CD34-enriched GFP-Tg ASC

2a). Immunophenotype of CD146$^-$ CD29$^+$, and CD146$^-$ CD34$^+$ sorted GFP-Tg ASC subpopulations. Immunophenotypes were based on expression of CD29, CD31, CD34, CD45, CD11B, Sca-1, and CD105 surface antigens. 2c). Adipogenic differentiation, and 2d) colony formation assays of unfractionated GFP-Tg ASC, CD146$^-$ CD29$^+$ GFP-Tg ASC, and CD146$^-$ CD34$^+$ GFP-Tg ASC. All experiments were repeated in triplicate; sample size, n=3 per replicate. Values reported as mean ± standard deviation (μ ± SD); *$p < 0.05$, ** $p < 0.01$; ***$p < 0.001$.

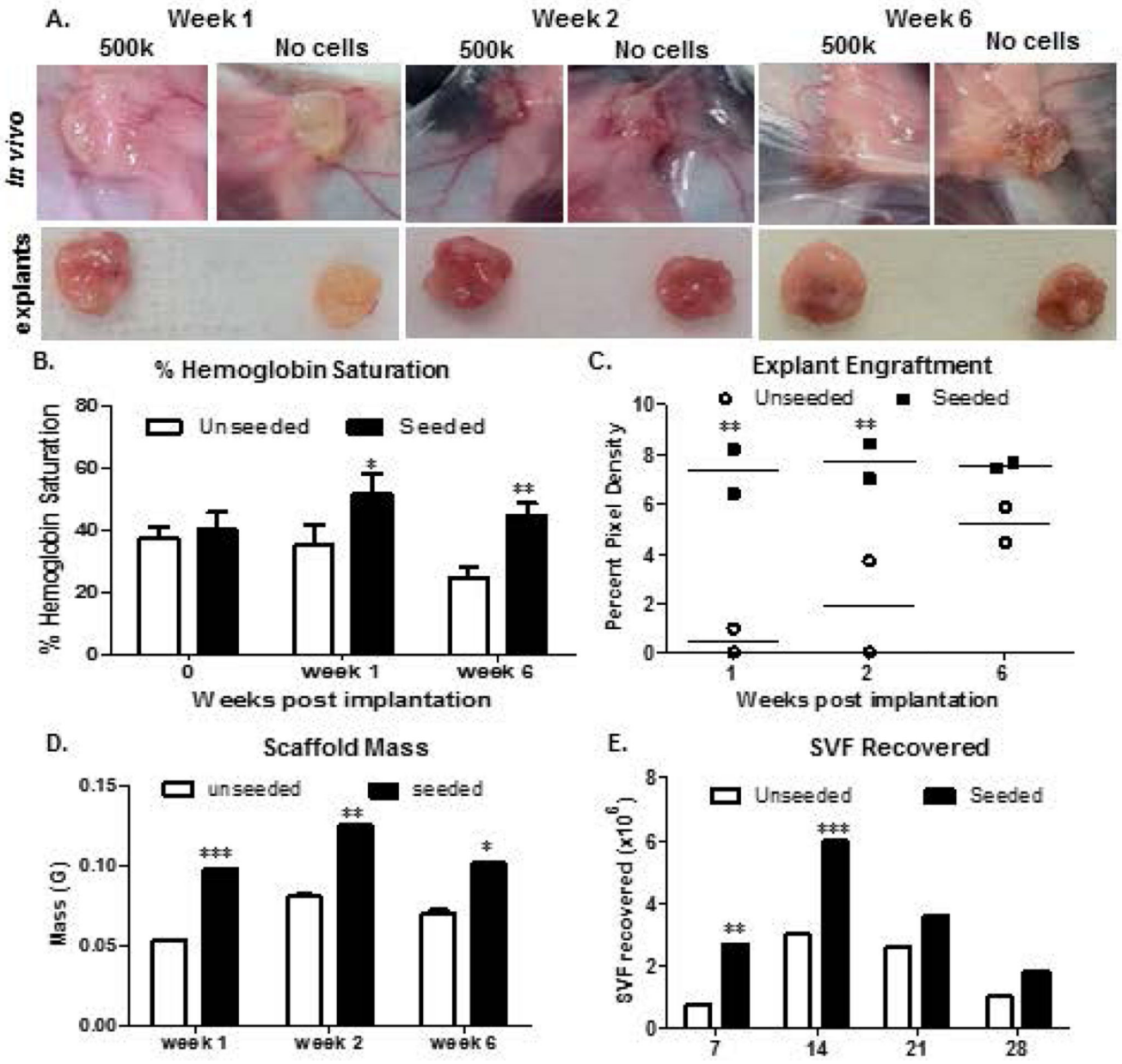

Figure 3. Weekly progression of tissue engineered fat within and surrounding GFP-Tg SVF cell implants in mice

3a). Scaffolds were implanted with no cells, or with 500k GFP-Tg SVF cells in silk scaffolds. Scaffolds were removed following 1 week, 2 weeks, or 6 weeks of implantation. 3b) Percent hemoglobin saturation was measured immediately following implantation, and after 1 week and 6 weeks of initial implantation. 3c). Quantification of removed scaffold (explant) engraftment via ImageJ analyses of photomicrographs in 3a; sample size, n=6 per group. 3d). Scaffold mass measurements following weeks 1, 2, and 6 of implantation; sample size, n=20. Quantification supports photomicrographs of SVF-mediated engraftment acceleration after 1 week of implantation. 3e). Weekly SVF cell quantification correlate with

SVF cell persistence and expansion by week 2, and differentiation. Values reported as mean ± standard deviation (μ ± SD); *p < 0.05, ** p < 0.01; ***p < 0.001.

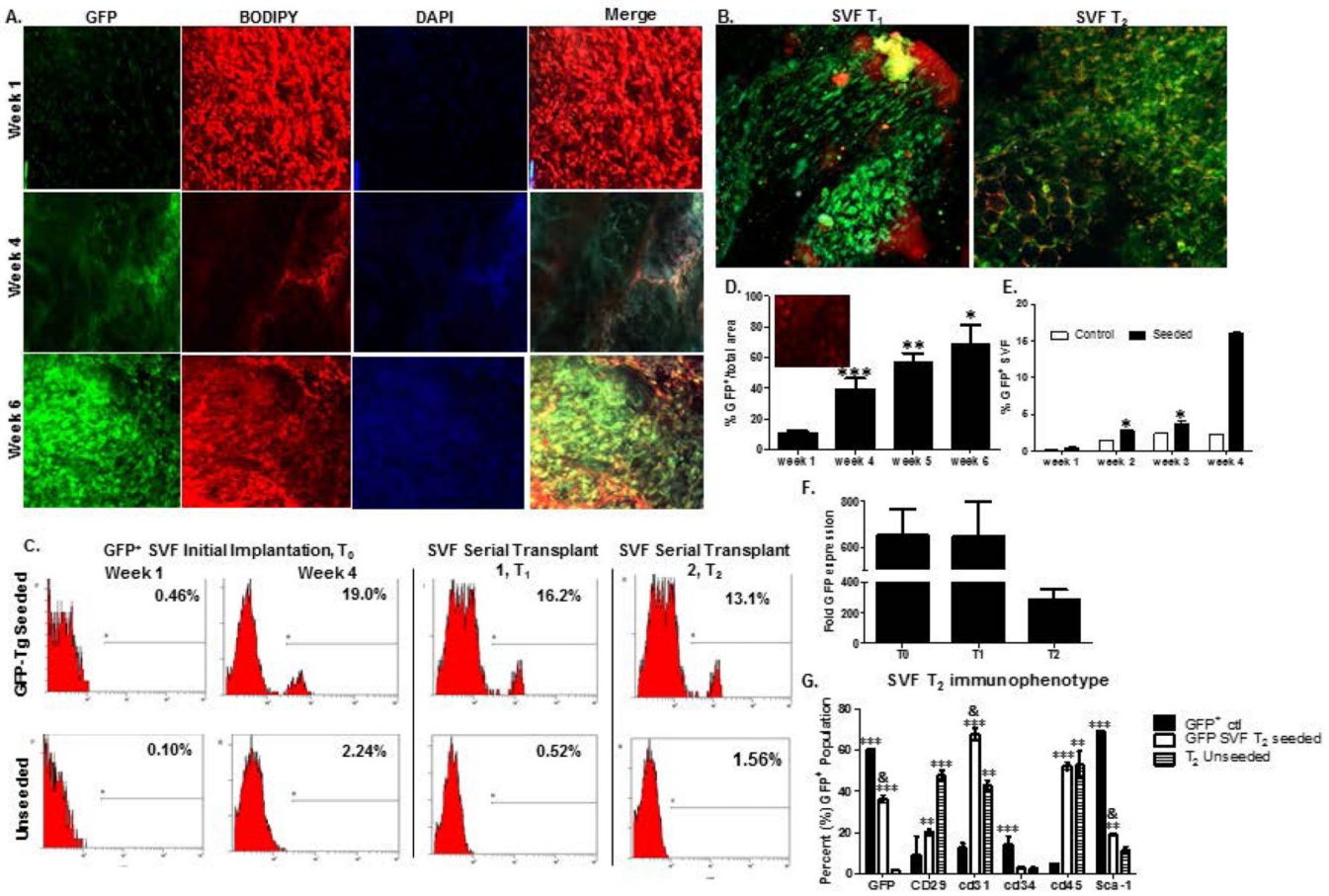

Figure 4. Detection of GFP-Tg SVF from tissue engineered adipose using HFIP 6-week silk scaffold implants in mice over two serial transplantations

Photomicrographs of GFP-Tg SVF cell implantation following weeks 1, 4, and 6 *in vivo* demonstrate persistence, proliferation, and ability to form GFP-Tg adipose depots. 4a). Confocal microscopy images of GFP, BODIPY, DAPI, and merged images within initial 6-week GFP-Tg SVF cell (T_0) transplants. 4b) Merged GFP/BODIPY/DAPI images of removed 6-week GFP-Tg SVF cell first serial (T_1) and second serial (T_2) transplants; sample size, n=5. 4c) Flow cytometric analyses of GFP expression in removed adipose scaffolds following T_0, T_1, and T_2 transplants; sample size, n=18. 4d). ImageJ analysis of weekly confocal images of T_0 explants. 4e) Quantification of weekly flow cytometric analyses of GFP expression in removed T_0 GFP-Tg SVF cell implants. 4f). GFP DNA expression in samples from removed 6-week T_0, T_1, and T_2 transplants. GFP expression reported as fold expression and normalized to GAPDH expression. 4g). Immunophenotype based on expression of GFP, CD29, CD31, CD34, CD45, and Sca-1 antigen expression on SVF cells isolated from 6-week T_2 transplants. Values reported as mean ± standard deviation (μ ± SD); comparing individual grouping to GFP^+ control: *$p < 0.05$, ** $p < 0.01$; ***$p < 0.001$; comparing to GFP-SVF T_2 seeded to unseeded control groups: $^{\&}$ $p < 0.05$.

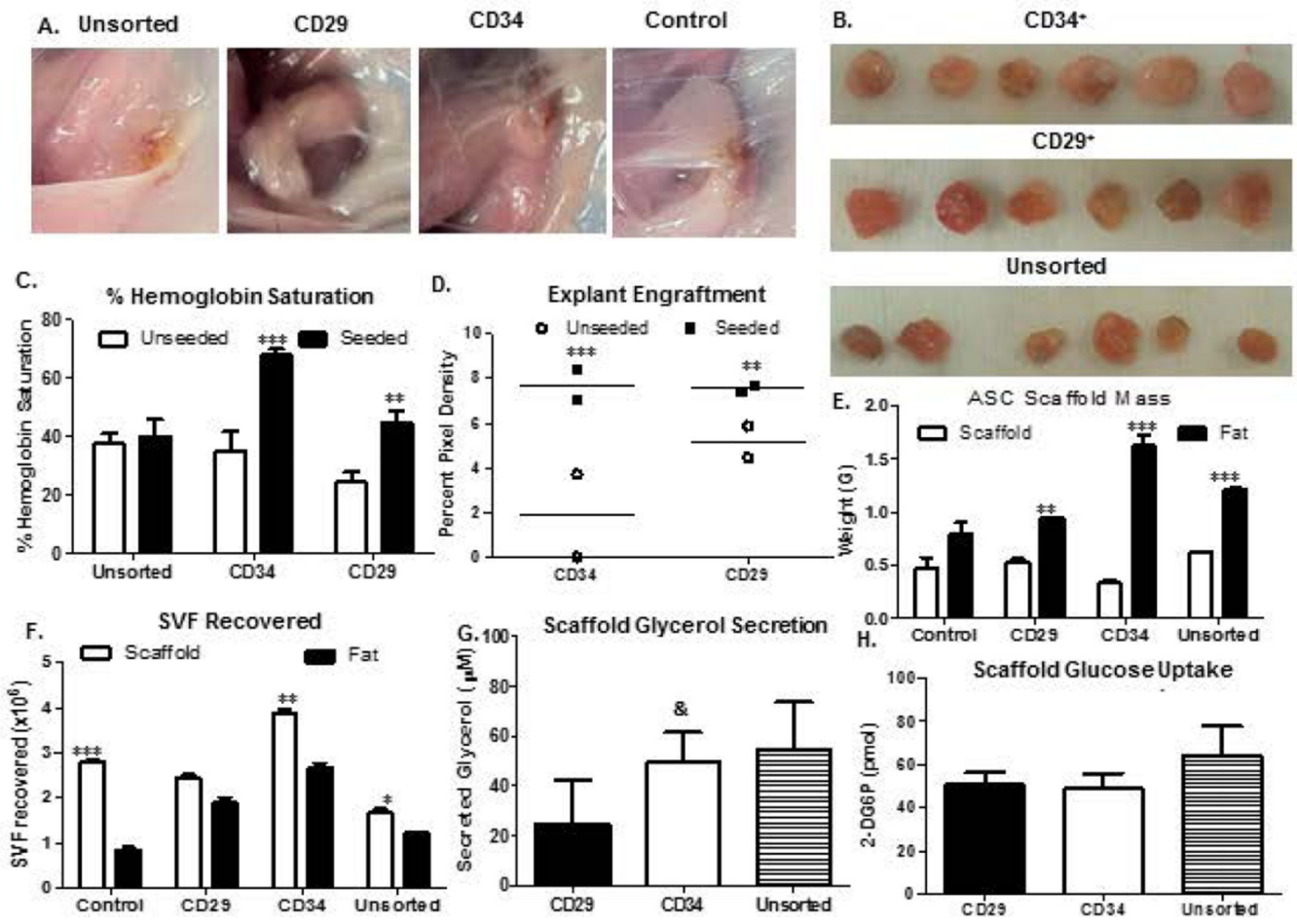

Figure 5. Adipose formation and functionality within GFP-Tg ASC seeded serial silk implants

5a). Photomicrographs of scaffolds that were implanted with no cells (control), or with (a), 500k unsorted GFP-Tg ASC; (b), $CD146^{-}$ $CD29^{+}$ GFP-Tg ASC; or (c), $CD146^{-}$ $CD34^{+}$ GFP-Tg ASC; in silk scaffolds. Scaffolds were removed following 6 weeks of implantation. 5b). Images of removed scaffolds from cohorts (a)-(c). 5c) Percent hemoglobin saturation was measured in groups (a)-(c) after 6 weeks of initial (T_0) implantation. 5d). Quantification of removed scaffold (explant) engraftment via ImageJ analyses of photomicrographs in 4b; sample size, n=6 per grouping. 5e). Scaffold mass measurements after 6-week implants of cohorts (a)-(c), and control implants that were not seeded with any cells. 5f). Quantification of SVF recovered from 6-week implants, and surrounding fat from cohorts (a)-(c), and the unseeded control group; sample size, n=18 per grouping. Functionality was measured via 5g) glucose uptake, and 5f) glycerol secretion assays using 6-week T_1 transplantation constructs. Data analyzed using Graphpad Prism. Two-way ANOVAs performed. Data reported as mean ± SD. *$p < 0.05$, ** $p < 0.01$; ***$p < 0.001$; comparing to CD34-enriched group: $^{\&}$ $p < 0.05$.

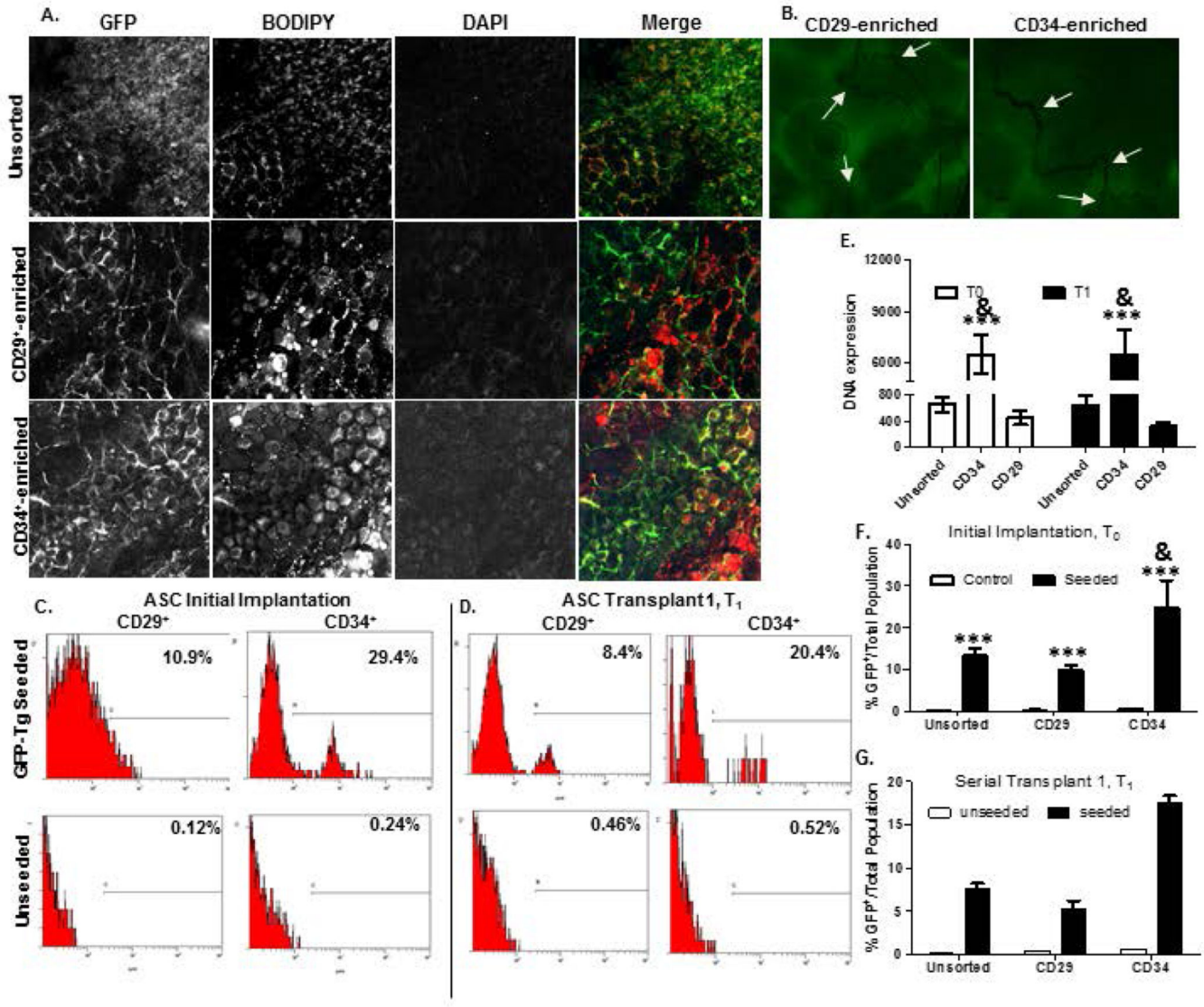

Figure 6. Detection of CD146^{-} CD29^{+} GFP-Tg ASC and CD146^{-} CD34^{+} GFP-Tg ASC from tissue engineered adipose using HFIP 6-week silk scaffold implants in mice over two serial transplantations

Photomicrographs of GFP-Tg CD29-enriched and CD34-enriched (cohorts (a)-(c) cell implantation following week 6 *in vivo* demonstrate persistence, proliferation, and ability to form GFP-Tg adipose depots, similar to unsorted GFP-Tg SVF cohorts. 6a). Confocal microscopy images of GFP, BODIPY, DAPI, and merged images from 6-week GFP-Tg ASC serial (T_1) transplants. 6b) Confocal images of CD29-enriched and CD34-enriched 6-week T_1 groups reflected observation of micro vessel formation within CD34-enriched groups than in CD29-enriched groups; n=5 per group per replicate. Flow cytometric analyses of GFP expression in removed adipose scaffolds from cohorts (a)-(c) following 6c) T_0, and 6d) T_1 transplants. 6e). GFP DNA expression in samples from removed 6-week T_0 and T_1 transplants. GFP expression reported as fold expression and normalized to GAPDH expression. Quantification of %GFP positivity following 6-week transplantation in 6f) T_0 and 6g) T_1 GFP-Tg ASC cell implants. Data reported as mean + SD. Comparing individual

grouping to unsorted cell seeded groups: *p < 0.05, ** p < 0.01; ***p < 0.001; comparing to CD34-enriched group: & p < 0.05

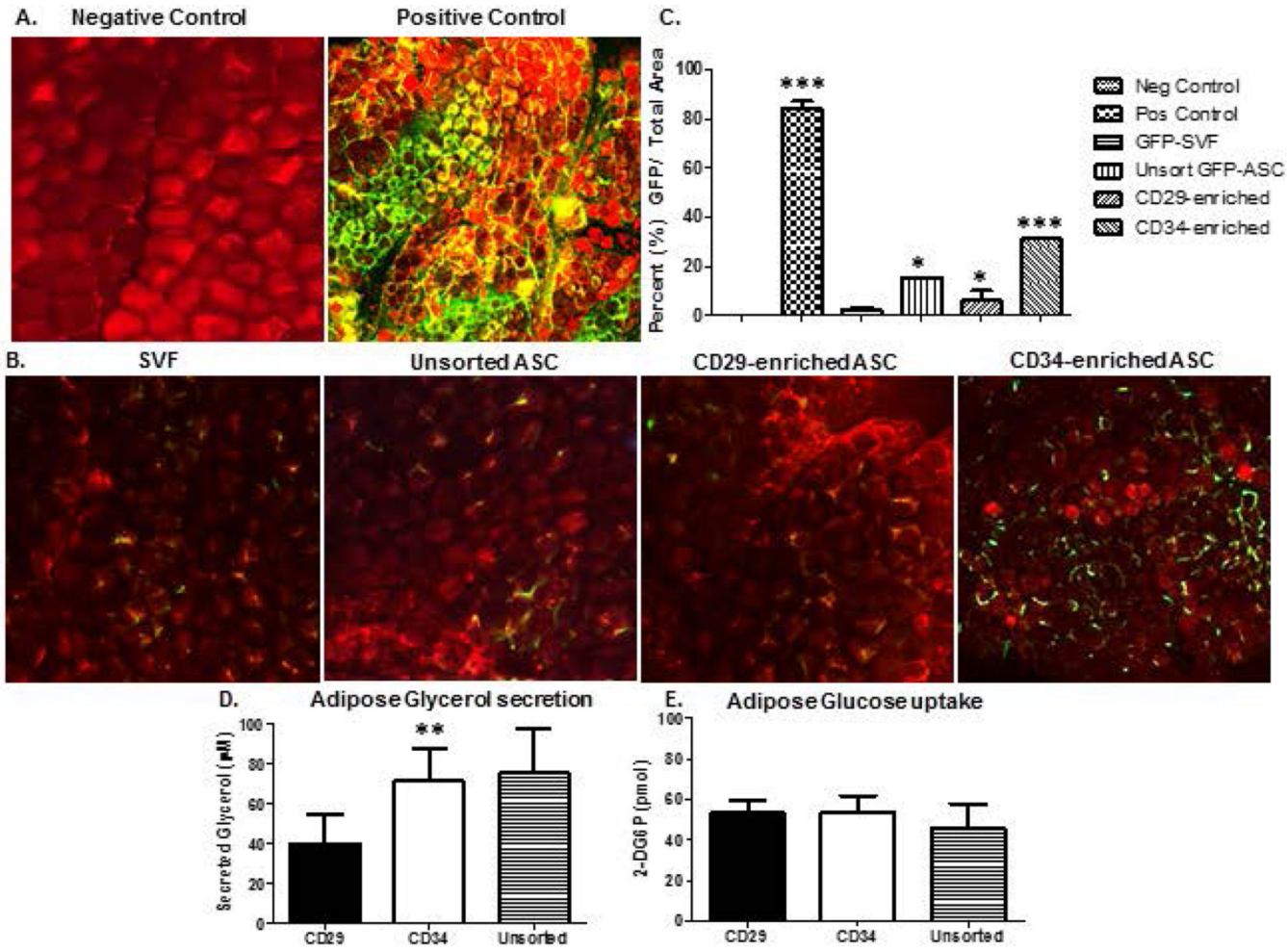

Figure 7. GFP-Tg SVF cells, CD29-enriched, and CD34-enriched GFP-Tg ASC infiltrate surrounding tissue to generate functional, GFP-Tg adipose

Confocal microscopic images of fat within 2mm surrounding SVF and ASC constructs revealed GFP positivity. 7a) Merged images of negative and positive control adipose stained with BODIPY and DAPI in non-GFP-Tg mice and GFP-Tg mice, respectively. 7b) Images of adipose surrounding 6-week constructs that were seeded with unsorted GFP-Tg SVF cells, unsorted GFP-Tg ASC, and CD146 CD29-enriched and CD34-enriched GFP-Tg ASC; n=5 per group per replicate. 7c) Quantification of confocal images from 7a and 7b. Functionality reported via 7d) glycerol secretion, and 7e) glucose uptake assays using 6-week T_1 transplantation constructs. Data reported as mean ± SD. *$p < 0.05$, ** $p < 0.01$; ***$p < 0.001$